HHS Public Access

Author manuscript

Acta Biomater. Author manuscript; available in PMC 2018 January 15.

Published in final edited form as:

Acta Biomater. 2017 January 15; 48: 258–269. doi:10.1016/j.actbio.2016.10.027.

Enzyme-mediated stiffening hydrogels for probing activation of pancreatic stellate cells

Hung-Yi Liu[1], **Tanja Greene**[2], **Tsai-Yu Lin**[2], **Camron S. Dawes**[2], **Murray Korc**[3,4], and **Chien-Chi Lin**[1,2,3,4,*]

[1]Weldon School of Biomedical Engineering, Purdue University, West Lafayette, IN 47907, USA

[2]Department of Biomedical Engineering, Purdue School of Engineering & Technology, Indiana University-Purdue University Indianapolis, Indianapolis, IN 46202, USA

[3]Department of Medicine and Biochemistry & Molecular Biology, Indiana University School of Medicine, Indianapolis, IN 46202, USA

[4]Indiana University Melvin and Bren Simon Cancer Center, Indianapolis, IN 46202, USA

Abstract

The complex network of biochemical and biophysical cues in the pancreatic desmoplasia not only presents challenges to the fundamental understanding of tumor progression, but also hinders the development of therapeutic strategies against pancreatic cancer. Residing in the desmoplasia, pancreatic stellate cells (PSCs) are the major stromal cells affecting the growth and metastasis of pancreatic cancer cells by means of paracrine effects and extracellular matrix protein deposition. PSCs remain in a quiescent/dormant state until they are ‘activated’ by various environmental cues. While the mechanisms of PSC activation are increasingly being described in literature, the influence of matrix stiffness on PSC activation is largely unexplored. To test the hypothesis that matrix stiffness affects myofibroblastic activation of PSCs, we have prepared cell-laden hydrogels capable of being dynamically stiffened through an enzymatic reaction. The stiffening of the microenvironment was created by using a peptide linker with additional tyrosine residues, which were susceptible to tyrosinase-mediated crosslinking. Tyrosinase catalyzes the oxidation of tyrosine into dihydroxyphenylalanine (DOPA), DOPA quinone, and finally into DOPA dimer. The formation of DOPA dimer led to additional crosslinks and thus stiffening the cell-laden hydrogel. In addition to systematically studying the various parameters relevant to the enzymatic reaction and hydrogel stiffening, we also designed experiments to probe the influence of dynamic matrix stiffening on cell fate. Protease-sensitive peptides were used to crosslink hydrogels, whereas integrin-binding ligands (e.g., RGD motif) were immobilized in the network to afford cell-matrix interaction. PSC-laden hydrogels were placed in media containing tyrosinase for 6 hours to achieve *in situ* gel stiffening. We found that PSCs encapsulated and cultured in a stiffened matrix

*To whom correspondence should be sent: Chien-Chi Lin, PhD., Associate Professor, Department of Biomedical Engineering, Purdue School of Engineering & Technology, Indiana University-Purdue University Indianapolis, Indianapolis, IN 46202, Phone: (317) 274-0760, lincc@iupui.edu.

expressed higher levels of αSMA and hypoxia-inducible factor 1α (HIF-1α), suggestive of a myofibroblastic phenotype. This hydrogel platform offers a facile means of *in situ* stiffening of cell-laden matrices and should be valuable for probing cell fate process dictated by dynamic matrix stiffness.

Graphical Abstract

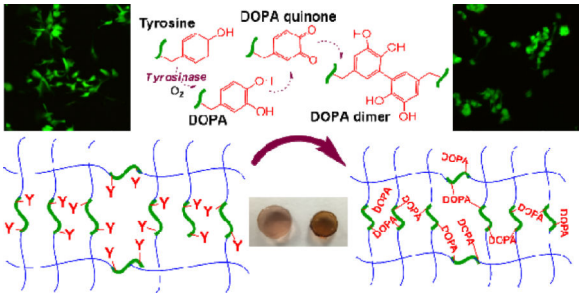

Keywords

hydrogels; tyrosinase; tissue stiffening; pancreatic cancer; stellate cells

1. Introduction

The stiffness of extracellular matrices (ECM) increase during the progression of many diseases, including cancers [1, 2]. The implications of a stiffened tissue include abnormal intracellular mechano-sensing and signal transduction, increased expression of ECM proteins, and durotaxis of cells (i.e., cell migration guided by gradients of matrix rigidity). Seminal works concerning the influence of matrix mechanics on cell fate processes relied largely on two-dimensional (2D) polyacrylamide hydrogels with surface-adsorbed or conjugated ECM proteins [3]. Culturing cells on a 2D surface, however, does not truly recapitulate the complex architecture of three-dimensional (3D) ECM [4]. In this regard, cell-laden hydrogels are increasingly being explored for modeling disease progression *in vitro* or *ex vivo*, as well as for regenerating tissues *in vivo*. The high water content and good permeability of a highly swollen hydrogel permits facile nutrient-waste exchange, whereas the crosslinked polymeric network gives rise to tunable elasticity and easy tethering of bioactive motifs for supporting cell survival and function in 3D [5]. Hydrogels prepared from synthetic polymers, such as poly(ethylene glycol) (PEG), are particularly suitable for investigating the influence of extracellular matrix mechanics on cell fate because the crosslinking density, and hence the stiffness, of a biomimetic hydrogel can be precisely engineered [5].

In recent years, hydrogels with dynamically tunable crosslinking kinetics are increasingly being explored for studying mechanobiology in 3D [6–8]. The general principle of designing a dynamic hydrogel is to perform cell encapsulation within a primary hydrogel network that allows for post-gelation modification in gel crosslinking density. Employing a two-stage crosslinking strategy, Burdick and colleagues showed that cell-laden hydrogels could be stiffened in a spatial-temporally controlled manner [8]. The hydrogels were first prepared by

thiol-based Michael-type addition between methacrylated hyaluronan (MeHA) and dithiothreitol (DTT) with an off-stoichiometric ratio. The excess methacrylate moieties in the primary hydrogel network permit subsequent light-and-radical-mediated chain-growth polymerization to produce a stiffened gel matrix. Anseth *et al.* showed that a stiffened hydrogel matrix could be achieved simply by performing a secondary step-growth photopolymerization in the presence of a pre-gelled cell-laden hydrogel network [9]. *In situ* hydrogel stiffening could also be achieved through light irradiation. For example, PEG-based hydrogels with azobenzene were prepared to undergo reversible swelling upon azobenzene *cis-trans* isomerization, which is induced by UV or visible light exposure, respectively [10]. Although the azobenzene-linker chain length, and hence hydrogel swelling, could be modulated by light exposure, the magnitude of gel modulus change was minimal and not physiologically relevant. Alternatively, infrared (IR)-induced heating was used to tune the stiffness of alginate hydrogels across a physiologically relevant range [11]. In this example, temperature-sensitive liposomes were loaded with gold nanorods as well as calcium, and were subsequently encapsulated in the alginate gels. Upon IR irradiation, the heated gold nanorods disrupt the liposomes, causing the release of calcium ions to induce gelation of alginate chains. Although IR light is considered safer than UV light, the generation of heat upon IR irradiation might not be ideal for certain applications. Our group has utilized host-guest (cyclodextrin-adamantane) interactions to reversibly tune the stiffness of cell-laden hydrogels across several hundreds to thousands of Pascals [12]. Collectively, these approaches provide a wide variety of options for irreversibly or reversibly tuning the stiffness of cell-laden hydrogels.

Owing to their substrate specificity and predictable enzymatic reaction kinetics, various enzymes (e.g., plasmin, transglutaminase, horseradish peroxidase, glucose oxidase, and tyrosinase) have been successfully used to induce gel crosslinking and, in some cases, cell encapsulation [13–17]. For example, tyrosinase (also named polyphenol oxidase) catalyzes the oxidation of phenol into dihydroxyphenylalanine (DOPA), DOPA quinone, and subsequently into DOPA dimer [18]. Tyrosinase-mediated reactions also consume molecular oxygen and produce water as the only by-product. Tyrosine or DOPA conjugated polymers (e.g., PVA, gelatin, dextran, etc.) are susceptible to tyrosinase-mediated crosslinking [19]. Due to its mild reaction conditions, tyrosinase is increasingly being explored for hydrogel crosslinking and *in situ* cell encapsulation [14]. To the best of our knowledge, however, tyrosinase-mediated DOPA crosslinking mechanism has not been exploited for *in situ* stiffening of cell-laden hydrogels. While tyrosinase-mediated DOPA formation was not found in the pancreatic tissue, this strategy provides facile, effective, and cytocompatible means of tuning matrix stiffness for *in vitro* or *ex vivo* tissue engineering applications.

In this contribution, we describe the design of orthogonally crosslinked PEG-peptide thiol-norbornene hydrogels susceptible to tyrosinase-mediated *in situ* gel stiffening. The primary hydrogel network was prepared by a light-mediated thiol-norbornene photopolymerization [20, 21] utilizing bis-cysteine-bis-tyrosine-bearing peptide crosslinkers. The pendant tyrosine residues in the primary step-growth hydrogel network permit additional crosslinking and gel stiffening triggered by the infiltration of tyrosinase. In addition to verifying the formation of DOPA crosslinks within a PEG-peptide hydrogel network, we also optimized the conditions for achieving a biologically relevant range of stiffening.

Finally, we utilized this *in situ* stiffening PEG-peptide hydrogel system to probe the effect of a stiffened matrix on the activation of pancreatic stellate cells.

2. Materials & Methods

2.1 Materials

Hydroxyl-terminated 8-arm PEG (20kDa) and 5-norbornene-2-carboxylic acid was obtained from JenKem Technology USA and Sigma-Aldrich, respectively. All reagents for chemical synthesis were purchased from Sigma-Aldrich unless otherwise noted. Reagents and Fmoc-amino acids for solid phase peptide synthesis were acquired from Anaspec or ChemPep.

2.2 Modeling of tyrosinase diffusion in hydrogels

The time-scale of tyrosinase diffusion into PEG-peptide hydrogel was estimated by Fick's 2nd Law of Diffusion in planar geometry (Equation 1) with appropriate initial (Equation 2) and boundary conditions (Equation 3, 4) as listed below:

$$\frac{\partial C_T}{\partial t} = D_T \frac{\partial^2 C_T}{\partial z^2} \quad (1)$$

$$@t=0\ C=0 \quad (2)$$

$$@z=0\ \frac{\partial C_T}{\partial z}=0 \quad (3)$$

$$@z=\pm h\ C_T=C_0 \quad (4)$$

Here, C_T and D_T are the concentration and diffusion coefficient of tyrosinase in a hydrogel, respectively; z is the coordinate perpendicular to the gel; t is the time of gel incubation in tyrosinase solution; *h* is the half-thickness of the gel; C_0 is the tyrosinase concentration in the buffer solution, which is assumed to be constant. Diffusion in this case was assumed to be symmetrical and only in the z-direction since the gels' diameter (~10 mm) was much greater than its thickness (<1 mm). Equations 1–4 were solved using Polymath software using a range of diffusion coefficients (~ 9×10^{-8} to 5×10^{-7} cm^2/sec) and gel thickness (~ 0.5 to 1 mm). The time needed for C_T at the center plane of the gel (i.e., z=0) to reach 99% of that in solution was plotted against the diffusion coefficient at a specific gel thickness.

The diffusion coefficient of tyrosinase is a function of hydrogel crosslinking density (ρ_x) and can be expressed using the Lustig-Peppas relationship [22]:

$$D_T(\rho_x) = D_{T,\infty} e^{-Y/(Q-1)} \left(1 - \frac{r_T}{\xi}\right) \quad (5)$$

Here, $D_{T,\infty}$ is the diffusion coefficient of tyrosinase in aqueous solution. Y is the critical volume (Y=1 for PEG-based gels) required for a successful translational movement of the substrate relative to the average free volume of a water molecule. ρ_x is the crosslinking density of the hydrogel dictated by the volumetric swelling ratio (Q) and mesh size (ξ) that are determined experimentally.

2.3 Macromer and peptide synthesis

Macromer eight-arm PEGNB (designated as PEG8NB) and photoinitiator lithium phenyl-2,4,6-trimethylbenzoylphosphinate (designated as LAP) were synthesized as described elsewhere [21, 23, 24]. The three MMP-sensitive bis-cysteine peptide crosslinkers, including KCGPQGIWGQCK, KCYGPQGIWGQYCK (designated as 2Y peptide), and YGKCYGPQGIWGQYCKGY (designated as 4Y peptide), were purchased from GenScript (purity > 90%). All other peptides, including CYGGGYC and CRGDS, were synthesized in an automated microwave-assisted peptide synthesizer (Liberty 1, CEM) using standard Fmoc coupling chemistry. Crude peptide was cleaved in a trifluoroacetic acid (TFA) cleavage cocktail, purified using reverse phase HPLC, and characterized by mass spectrometry. The purity of peptides was at least 90%.

2.4 Thiol-norbornene hydrogel crosslinking

The crosslinking of thiol-norbornene hydrogels was initiated by 365 nm light exposure and with 1 mM LAP as the photoinitiator. PEG8NB (Fig. 1A), bis-cysteine peptide crosslinker (e.g., CYGGGYC, Fig. 1B), and LAP at desired concentrations were mixed in phosphate-buffered saline (PBS) and irradiated under 365 nm light (5 mW/cm^2) for 2 minutes (Fig. 1C). For all gel formulations, the stoichiometric ratio of thiol to norbornene was maintained at one to afford the highest degree of gel crosslinking. Gels were maintained in DPBS at 37°C for at least 24 hours prior to characterization or stiffening experiments.

2.5 Tyrosinase-mediated *in situ* gel stiffening and characterization

Hydrogels were formed and swollen for 24 hours in PBS at 37°C, followed by incubation in tyrosinase solution for 6 hours. Afterwards, gels were transferred to PBS. Hydrogel elastic moduli (G' & G") before and after tyrosinase-mediated stiffening were obtained using oscillatory rheometry in strain-sweep mode (8 mm parallel plate geometry with a gap size of 750 μm). Due to volumetric shrinkage after stiffening, the gap size was reduced to 550 μm when measuring moduli of the stiffened hydrogels. The reported gel elastic moduli were averaged from the linear region of the modulus-strain curves.

2.6 Proteolytic degradation of stiffened hydrogels

Collagenase was used to evaluate the susceptibility of tyrosinase-stiffened hydrogels to protease-mediated gel degradation. Hydrogels were prepared and stiffened as described in the sections above. The stiffened hydrogels were incubated in PBS for two days, followed by

collagenase-1 (40 U/ml) mediated degradation. At pre-determined time intervals, the gels were removed from the protease solution, blotted dry, and weighed to determine the % mass loss, which is defined as the percentage of weight loss at each time interval to the initial weight obtained before protease treatment. The process was repeated until the gels were fully degraded.

2.7 Oxygen detection

Solution oxygen contents were recorded with an oxygen microsensor (MicroX4, PreSens) at specific time points during *in situ* stiffening. For this experiment, hydrogels were prepared using sterile-filtered macromers, MMP-sensitive peptides, photoinitiator, and tyrosinase. After thiol-ene gelation, the hydrogels were incubated in PBS for a day at 37°C before transferring to complete PSC culture media (ScienCell). Oxygen content before and after tyrosinase treatments were recorded periodically for 7 days.

2.8 Human pancreatic stellate cell (PSC) culture and encapsulation

Primary human pancreatic stellate cells (PSC or HPSteC) were obtained from ScienCell Research Laboratories and maintained in stellate cell media supplemented with 2% fetal bovine serum (FBS), antibiotics, and growth supplements (ScienCell). The cells were cultured on poly-L-lysine (PLL) coated plates according to the manufacturer's protocol. Cell culture media were refreshed every 2–3 days. Prior to encapsulation, cells were detached from the plate by trypsin-EDTA treatment for 3 minutes. Trypsin was neutralized with equal volume of media and transferred into 5 mL of FBS pre-warmed to room temperature. Trypsinized cells were centrifuged at 1000 rpm for 5 minute, counted, and mixed with sterile-filtered pre-polymer solutions (PEG8NB, peptide crosslinker (e.g., MMP-sensitive linker: KCGPQGIWGQCK), 1 mM CRGDS, and 1 mM LAP). Twenty-five microliter (25 μL) of the cell-polymer mixtures were transferred to a 1 mL syringe (tip cut open for solution loading and gel removal) and placed under 365 nm light tube in an aseptic laminar flow hood for *in situ* gel crosslinking and cell encapsulation. The encapsulation was achieved within 2 minutes. In all experiments, cells were encapsulated with a cell density of 1 million cells/mL. After encapsulation, cell-laden hydrogels were maintained in complete stellate cell medium and placed in a CO_2 incubator. Cell culture media was refreshed every 2–3 days.

2.9 *In situ* stiffening of cell-laden hydrogels and characterization of cell viability and morphology

To induce *in situ* stiffening, cell-laden hydrogels were transferred to a 48-well plate with wells containing cell media supplemented with 1 kU/mL tyrosinase. Gels were incubated for 6 hours at 37°C in 5% CO_2. Following the stiffening process, cell-laden hydrogels were transferred to and maintained in a 24-well plate containing only cell culture media. Encapsulated PSCs were stained with live/dead staining kit (Life Technologies) and imaged via confocal microscopy (Olympus Fluoview FV100 laser scanning microscope). To qualitatively assess the viability of the cells, z-stack images (100 μm thick, 10 μm per slice) were obtained from a minimum of three random fields of view for all experiments. Cell viability was also quantitatively assessed using AlamarBlue® reagent. In brief, cell-laden hydrogels were incubated in 500μL of cell culture media diluted by 1:10 dilution of the

reagent for 2.5 hours. Following incubation, 200μL of diluted media was transferred to a clear 96-well microplate, and the resulting fluorescence from the cells within hydrogels was determined by a microplate reader (SynergyHT,BioTek; ex 560 nm, em 590 nm).

F-actin staining was conducted to visualize cell spreading. Briefly, encapsulated cells were fixed in 4% paraformaldehyde for 1 hour at room temperature on an orbital shaker. Following fixation, hydrogels were washed with DPBS (2× at 10 minutes each) and permeabilized using 100× dilution of saponin (100 mg/mL in DMSO) in DPBS for 1 hour, followed by two successive washes in DPBS for 10 minutes each. Cell-laden gels were then incubated overnight at 4°C in DPBS solution containing 100 nM working solution of rhodamine phalloidin (f-actin cytoskeleton) and a 1:10000 dilution of DAPI (cell nuclei). On the day of imaging, cell-laden gels were washed three times in DPBST (DPBS with 1vol% of Tween 20) and imaged with confocal microscopy as described above. Cell spreading was quantified using three different fields for each condition. The perpendicular major (length) and minor (width) axes of individual cells were measured using Nikon imaging software (NIS-Elements) and length to width aspect ratios were determined. For each condition the total number of cells assessed ranged from 75 to 90 cells. GraphPad Prism 5 software was used to determine the cumulative distribution of aspect ratios collected.

2.10 RNA isolation, reverse transcription, and quantitative real time PCR

On predetermined days, hydrogels containing encapsulated PSCs were collected, placed in DNase/Rnase-free microtubes, and flash frozen using liquid nitrogen. Samples were then stored at −80°C until use. To extract RNA, frozen gels were homogenized in 600 μL of lysis buffer (NucleoSpin RNA II kit, Clontech) and were subjected to two additional cycles of freeze-thaw in order to lyse cells. Lysates were purified using NucleoSpin Filters. Following purification, 600 μL of Rnase-free 70% ethanol was added to the lysates and mixed thoroughly. The mixtures were then transferred to NucleoSpin RNA columns for RNA extraction following manufacturer's protocol. Using 30 μL of Dnase/Rnase-free water, the isolated RNAs were eluted and then quantified by UV spectrometry (NanoDrop 2000, Thermo Scientific). Using PrimeScript RT reagent kit (Clontech) the total isolated RNA were converted into single-stranded cDNA. Gene expression level was assessed by quantitative real-time PCR and analyzed following a published protocol. Real-time PCR primer sequences can be found listed in Table S1.

2.11 Statistics

Statistical analyses were conducted by Two-Way ANOVA followed by Bonferroni's post-hoc test using GraphPad Prism 5 software. The control group was specified in the respective figure caption. All experiments were conducted independently for at least three times and data presented were Mean ± SEM. Single, double, and triple asterisks represent $p<0.05$, 0.001, and 0.0001, respectively. $p<0.05$ was considered statistically significant.

3. Results & Discussion

3.1. Design principles of enzyme-mediated *in situ* stiffening of PEG-peptide hydrogels

Compared with the relatively heterogeneous chain-polymerized gels, step-polymerized hydrogels possess increased network homogeneity and mechanical integrity [25]. Here, we prepared the primary PEG-peptide hydrogel with orthogonal crosslinks and homogeneous network structure using PEG8NB (Figure 1A) and a model peptide CYGGGYC (Figure 1B). The basic peptide design rationale was to incorporate two terminal cysteines to permit light-mediated orthogonal thiol-norbornene step-polymerization (Figure 1C), as well as two pendant tyrosines to allow tyrosinase-mediated DOPA dimer formation (Figure 1D). The DOPA dimers formed within a covalently crosslinked hydrogel network would lead to an increased hydrogel crosslinking density, and hence a stiffened matrix. In principle, the step-polymerized PEG-peptide hydrogel can be stiffened at any point in time post-gelation by placing the hydrogels in a solution containing tyrosinase (Figure 1E). The degree of gel stiffening is dictated by the diffusion of tyrosinase into the hydrogel network, as well as the enzymatic reaction between infiltrated tyrosinase and pendant tyrosine residues. For most gel formulations used in this study, the concentration of the pendant tyrosine is fixed (i.e., 10 mM tyrosine for 2.5wt% $PEG8NB_{20kDa}$, $R_{[thiol]/[ene]} = 1$). Therefore, the formation of DOPA dimer and therefore the degree of hydrogel stiffening, depends largely on the availability of tyrosinase.

Fick's 2nd Law of Diffusion was used to estimate the time scale of tyrosinase diffusion in the hydrogel (Experimental Section, Equations 1–4). Two parameters are of utmost importance: the thickness of the hydrogel (h) and the diffusivity of tyrosinase (D_T). Gel thickness is easily controlled during hydrogel fabrication (typically between 0.5 mm to 1 mm), whereas D_T in hydrogel is affected by hydrogel crosslinking density and can be estimated using a free-volume approach described by Lustig and Peppas (Equation 5) [22]. The purpose of this modeling was to understand the minimal time needed for the hydrogel to be equilibrated with the enzyme. Therefore, the enzymatic reaction is not considered in this modeling and future work will focus on developing a comprehensive diffusion-reaction model to predict the degree of gel stiffening.

Depending on its size, the diffusivity of a protein in a highly swollen hydrogel is estimated to be about 20–80% of its value in aqueous solution [26, 27]. Since the diffusivity of tyrosinase (MW: 128kDa) in water has been determined to be ~5×10^{-7} cm^2/sec [28], the possible range of tyrosinase diffusivity in the highly swollen PEG-peptide hydrogels should be 1×10^{-7} to 4×10^{-7} cm^2/sec. This assumption was also supported by our determination of tyrosinase diffusivity in either non-stiffened or stiffened hydrogels (i.e., 3×10^{-7} to 4×10^{-7} cm^2/sec. see Figure S1). Fick's 2nd Law of Diffusion in planar geometry (Equations 1–4) was used to estimate the time scale of tyrosinase diffusion in the highly swollen PEG-peptide hydrogel. As shown in Figure 1F, the minimal time required to achieve 99% ($T_{99\%}$) of equilibrium tyrosinase concentration at the center of the hydrogel (i.e., $C_{T,z=0}/C_{T,z=h}$ = 99%) is governed by the diffusivity of tyrosinase and the thickness of the hydrogel. From the numerical solutions, we randomly selected $T_{99\%}$ = 6 hours to gauge the relative influence of h and D_T on tyrosinase diffusion in hydrogels. Intuition suggests that h is positively

correlated to $T_{99\%}$, while D_T is negatively correlated to $T_{99\%}$. Indeed, we found that when the gel is thin (e.g., $h = 0.5$ mm), $T_{99\%}$ is much shorter than 6 hours regardless of D_T (regions 1 & 2). On the other hand, when the gel is thicker (e.g., $h = 1$ mm), $T_{99\%}$ is highly dependent on D_T, which is governed by hydrogel crosslinking density. For example, $T_{99\%}$ is under 6 hours if the crosslinking density of a 1 mm thick gel is adjusted such that D_T is greater than 2.05×10^{-7} cm^2/sec (region 1). On the other hand, $T_{99\%}$ is longer than 6 hours if the crosslinking density of the 1 mm-thick hydrogel is high enough to decrease D_T to below 2.05×10^{-7} cm^2/sec (region 3). The modeling results shown in Figure 1F suggest that the degree of tyrosinase-mediated gel stiffening should be highly effective for thin hydrogels ($h < 0.5$ mm) and for thick hydrogels (e.g., $h \sim 1$ mm) with lower crosslinking density. Furthermore, our estimation of tyrosinase diffusivity in non-stiffened or stiffened hydrogels (i.e., 3×10^{-7} to 4×10^{-7} cm^2/sec. Equation 5 and Figure S1) suggested that 6 hours of incubation was sufficient for the hydrogels (actual thickness ~1 mm) to be equilibrated with tyrosinase (region 1). While this model prediction did not take into account enzymatic reaction, the results nonetheless provide general guidance for fabricating the primary hydrogel network.

3.2 Tyrosinase-mediated *in situ* stiffening of step-polymerized PEG-peptide hydrogels

Prior to testing the hypothesis that tyrosinase could be used to stiffen hydrogels crosslinked by bis-tyrosine-bearing peptide (e.g., CYGGGYC), we first examined the formation of DOPAs from tyrosinase-mediated oxidation of soluble model peptide CYGGGYC. Scanning of UV/Vis absorbance from 250–500 nm demonstrated the formation of DOPAs. As shown in Figure 2A, solution containing only the model peptide CYGGGYC exhibited strong absorbance at 280 nm. Immediately upon the addition of 1 kU/mL tyrosinase into the peptide solution (e.g., Peptide+Tyrosinase, 0-hr), the observed peak absorbance redshifted slightly to 285 nm and an absorbance shoulder between 300–500 nm emerged. After 24 hours of incubation, the peak absorbance redshifted further to 295 nm, and the absorbance shoulder became even more pronounced. The absorbance redshift could also be easily observed in the peptide/tyrosinase solutions. As the incubation time was increased, the color of the solution turned from light yellow to dark brown (data not shown). As previously reported, the redshift in absorbance and the emergence of dark brown color are clear indications that DOPA are formed in the solution [29].

After confirming that tyrosine-containing peptides could be oxidized into DOPAs by tyrosinase, we sought to test whether the same phenomenon would occur in bis-tyrosine-containing peptide crosslinked PEG8NB hydrogels, which were polymerized from light initiated thiol-norbornene photo-click reaction using 2.5 wt% $PEG8NB_{20kDa}$ and 5 mM CYGGGYC ($R_{[thiol]/[ene]}=1$). After swelling for 24 hours, hydrogels were placed in buffer solution containing different concentrations of tyrosinase (i.e., 0, 0.01, 0.1, and 1 kU/mL) for 6 hours. As shown in Figure 2B, the hydrogels incubated in 0 and 0.01 kU/mL tyrosinase remained transparent. On the other hand, the color of gels incubated in 0.1 and 1 kU/mL tyrosinase turned to light yellow and brown, respectively. Since tyrosine residues were immobilized in the hydrogel network, the darker color formed in the initially transparent hydrogels indicated the formation of DOPAs. Furthermore, the diameter of the hydrogel incubated in 1 kU/mL tyrosinase reduced about 20%, suggesting shrinkage of the hydrogel

upon the formation of DOPAs in the hydrogel network. Finally, we evaluated the shear moduli (G') of these hydrogels (Figure 2C) and found that gels incubated in 0 and 0.01 kU//mL tyrosinase for 6 hours showed no difference in moduli before and after incubation (i.e., 0, 2, and 6 hours). The moduli remained similar after prolonged incubation in PBS for another 18 hours and 42 hours (i.e., total time 24 and 48 hours). For gels incubated in 0.1 kU/mL tyrosinase, however, moduli increased rapidly from 500 Pa to respectively 1,200 Pa and 1900 Pa after 2 hours and 6 hours of tyrosinase incubation. After 6 hours of incubation, gels were again moved to PBS for another 18 hours and 42 hours (i.e., total time 24 and 48 hours) and the moduli remained at around 1,900 Pa to 2,000 Pa. The stiffening effect after tyrosinase incubation suggests that DOPA formed in the hydrogel network led to increased crosslinking density. Similar phenomenon occurred in gels incubated in 1 kU/mL tyrosinase, except that the increases in moduli were even higher (to more than 3,100 Pa). Interestingly, the moduli increased for another 200–400 Pa after the gels were transferred to PBS, indicating that tyrosinase retained in the hydrogel continued to crosslink tyrosine residues after the gels were transferred to PBS. In addition, hydrogels pre- and post-stiffening (by 1 kU/mL tyrosinase) did not exhibit noticeable stress relaxation (Fig. S2) since both the primary and secondary crosslinks (i.e., thioether bonds and DOPA dimers) were all covalent bonds. These results show that tyrosinase indeed could be used to effectively stiffen hydrogels containing pendant tyrosine residues. Through simple peptide sequence design (i.e., adding additional tyrosine residues) and exogenously adding tyrosinase, we have achieved tunable *in situ* gel stiffening. Although tyrosinase has been used to crosslink DOPA-bearing macromers into hydrogels [13, 14], we believe the present work represents the first example of using tyrosinase to tune matrix stiffness.

3.3 Controlling the degree of *in situ* gel stiffening

In addition to adjusting enzyme concentration and incubation time, we also evaluated the effect of initial gel crosslinking density on the degree of *in situ* gel stiffening. Figure 3A shows the results of tyrosinase-mediated *in situ* gel stiffening using PEG8NB at three weight percentages during gel crosslinking (2.5 wt%, 3.0 wt%, and 3.5 wt%). As expected, gels crosslinked with higher weight percent of PEG8NB were stiffer following thiol-norbornene photo-crosslinking (~800 Pa, 1,800 Pa, and 2,800 Pa for 2.5 wt%, 3.0 wt%, and 3.5 wt%, respectively). After 6 hours of tyrosinase treatment (0.1 kU/mL), hydrogels had various degree of stiffening where stiffer gels exhibited moderate degrees of stiffening (~1.8-fold, 1.3-fold, and 1.1-fold increase in G' for 2.5 wt%, 3.0 wt%, and 3.5 wt%, respectively). The decreases in the degree of stiffening at higher weight percent PEG hydrogels could be attributed to the hindered tyrosinase diffusion in highly crosslinked gels. This shortcoming, however, could be circumvented by using a higher concentration of tyrosinase (Figure 2C). Figure 3B shows that the degree of stiffening could be tuned by mixing peptides without tyrosine in its sequence. As expected, hydrogels crosslinked with 100% tyrosinase-sensitive peptide (i.e., CYGGGYC) showed the highest degree of stiffening. The degree of gel stiffening in gels crosslinked by 50% CYGGGYC peptide fell in between gels crosslinked by 100% and 0% CYGGGYC peptide. The moduli of gels crosslinked with purely tyrosinase-insensitive CGGGC peptide remained relatively unchanged after tyrosinase treatment. Finally, we examined whether the stiffening process could be temporally controlled. At day-1 post-gelation, PEG8NB-CYGGGYC hydrogels were incubated in 0.1

kU/mL tyrosinase solution for 3 hours and once again at day-3 post-gelation (Figure 3C). Although a step-wise increase in gel stiffness was observed, the degree of stiffening was lower after the second tyrosinase treatment. It is also worth noting that between the two tyrosinase treatments, gel moduli gradually increased, which again was a result of residual reactivity from tyrosinase trapped in the hydrogel.

3.4 Designing stiffening hydrogels with protease-sensitivity

The design of hydrogels for cell encapsulation often requires incorporating integrin-binding and protease-cleavable motifs that permit cell binding to the matrix and protease-mediated cleavage of the pericellular matrix, respectively [30, 31]. These motifs have proven critical in cell migration, proliferation, and differentiation. For thiol-norbornene hydrogels, integrin-binding motifs are commonly incorporated as pendant peptides (e.g., CRGDS), whereas protease-cleavable motifs are incorporated as hydrogel crosslinkers [20, 21, 32, 33]. Based on this design principle, we used three versions of protease-cleavable peptide crosslinkers, including regular MMP-sensitive peptide without tyrosine residues (designated as 0Y, sequence: KCGPQGIWGQCK), and MMP-sensitive peptide with two or four tyrosine residues (designated as 2Y (Figure 4A) and 4Y (Figure 4B), respectively). These peptides also contain two cysteine residues that are essential in thiol-norbornene gel crosslinking. Since these peptides will be used for cell encapsulation, we tested whether gels crosslinked by 2Y peptide were susceptible to tyrosinase-mediated *in situ* stiffening in cell culture media (CM). We found that, while PEG-2Y hydrogels were stiffened by 0.1 kU/mL tyrosinase in both PBS and in CM, the degree of stiffening in CM was much less than that in PBS (Figure 4C) at the same tyrosinase concentration (i.e., 0.1 kU/mL). This deficit, however, could be easily rectified by using a higher concentration (i.e., 1 kU/mL) of tyrosinase (Figure 4C). In this study, we still observed increases in gel moduli after the gels were transferred to PBS. This phenomenon, however, was less apparent when the gels were transferred to tyrosinase-free CM (Figure 4C). The decreased responsiveness in tyrosinase-mediated stiffening in CM suggested that the components in serum-containing CM might hinder enzymatic reaction.

We also explored *in situ* gel stiffening using different tyrosine-containing peptides. Specifically, 2Y and 4Y peptides were used to crosslinked PEG8NB, and the resulting gels were stiffened using 1 kU/mL tyrosinase in CM for 6hr. Since the concentration of tyrosine residues in PEG8NB-4Y hydrogels was two-fold higher than that in PEG8NB-2Y hydrogels, it was not a surprise to obtain almost a two-fold difference in the degree of stiffening when 4Y peptide was used. This study demonstrated that the tyrosinase-mediated gel stiffening could be achieved through the adjustment of multiple parameters, including the content of macromer or tyrosinase-sensitive peptide in the hydrogels, or simply through using peptides with a higher number of tyrosine residues.

3.5 Proteolytic degradation of stiffened hydrogels

Proteolytic susceptibility of a biomimetic hydrogel supports various aspects of cell fate processes. Here, we demonstrated that PEG8NB-peptide hydrogels stiffened by tyrosinase were still susceptible to collagenase mediated proteolysis. Figure 5A shows the timeline of the stiffening and degradation study using PEG8NB hydrogels crosslinked by either 2Y or 4Y MMP-sensitive peptide (Figures 4A, 4B). Figures 5B and 5C show the profiles of

collagenase induced mass loss of PEG-2Y and PEG-4Y hydrogels without (Figure 5B) and with (Figure 5C) tyrosinase-mediated *in situ* gel stiffening. Similar to data reported in literature, non-stiffened hydrogels crosslinked by MMP-sensitive peptide started to lose mass as soon as the gels were placed in collagenase solution [21, 34]. Furthermore, the mass loss profiles exhibited good linearity with time owing to the step-polymerized hydrogel network structure [34]. Interestingly, the gels crosslinked by 4Y peptide appears to degrade slower than those crosslinked by 2Y peptide. We reason that the delayed proteolysis in PEG-4Y hydrogels was due to the presence of additional aromatic tyrosine residues that reduced the accessibility of collagenase to the MMP-sensitive peptide sequence, as the swelling ratio (Figure S2A), mesh size (Figure S2B), and diffusion coefficient (Figure S2C) of the two sets of hydrogels appeared to be very similar before tyrosinase-mediated stiffening. The degradation profiles of tyrosinase-stiffened hydrogels (Figure 5C), on the other hand, were drastically different than their non-stiffened counterparts. Although collagenase treatment still caused changes in gel mass, the hydrogels actually gained weight (i.e., negative mass loss) during the first two days; after which, the gels started to lose mass (i.e., positive mass loss). We have previously described similar degradation profiles in highly crosslinked gelatin-based thiol-norbornene hydrogels [35]. We reason that the initial mass gain in stiffened hydrogela was due to partial network cleavage that allowed water infiltration. Since the stiffened hydrogels were composed of thiol-norbornene crosslinks and DOPA dimer crosslinks, simply cleaving the peptide linker was not sufficient to cause gel mass loss. Therefore, a longer incubation time (>2 days) was required to cause positive gel mass loss. Furthermore, PEG-4Y hydrogels exhibited less responsiveness to collagenase-mediated degradation. This was again attributed to the potential decrease in collagenase accessibility to its peptide substrate due to the presence of additional DOPA crosslinks; because both stiffened PEG-2Y and PEG-4Y hydrogels had similar gel properties (Figure S1). Although the proteolytic degradation profiles were different in non-stiffened and stiffened hydrogels, this study nonetheless demonstrated that tyrosinase-stiffened hydrogels were still susceptible to proteolytic degradation. Furthermore, the delayed degradation behavior in stiffened hydrogels may more closely resemble a stiffened tumor matrix.

3.6 Probing the effect of *in situ* gel stiffening on myofibroblastic activation in human pancreatic stellate cells

We have previously reported the use of biomimetic PEG-peptide hydrogels for studying pancreatic cancer cell growth, morphogenesis, and drug sensitivity [33]. The diagnosis and treatments of pancreatic cancer remain difficult owing to the complicated interactions between various components in the pancreatic tumor mass, including primary tumor cells, stromal cells (e.g., stellate cells, cancer associated fibroblasts), immune cells, cytokines, proteases (e.g., matrix metalloproteinases or MMPs), and ECM proteins (e.g., collagen, fibronectin, laminin, etc.) [2]. Experimental evidence suggests that activated PSCs are the major stromal cells that secrete cytokines to enhance proliferation of primary tumor cells and increase their metastasis potential through epithelial-mesenchymal transition (EMT) [36, 37]. Activated PSCs become cancer associated fibroblasts (CAFs) which are responsible for depositing and organizing ECM proteins, such as collagen and laminin, leading to the stiffening of the local desmoplasia. PSCs remain in a quiescent/dormant state until they are ‘activated’ by various environmental cues whose identities are gradually being identified

[36, 37]. For example, PSCs are activated by transforming growth factor β (TGF β) through Smad2/3 phosphorylation.[38] TGFβ-activated PSCs express a higher content of α smooth muscle actin (αSMA), which leads to increased intracellular cytoskeletal tension and myofibroblast-like contractile phenotype. In spite of its potential importance, the influence of matrix stiffness on PSC activation is largely unexplored.

We utilized human pancreatic stellate cells (PSC) as a model to evaluate the biological relevance of tyrosinase-mediated gel stiffening strategy. Prior to the stiffening experiments, we demonstrated that regular thiol-norbornene PEG-peptide hydrogels formed with different stiffness (2.5–4 wt% PEG8NB) were cytocompatible for *in situ* encapsulation of PSCs (Figure S3). The cells were able to survive for at least one week in the hydrogels with soft (2.5 wt%) and stiff (4 wt%) hydrogels, as demonstrated by the steady increase in metabolic activity (Figure S4). However, cells grown in stiff hydrogels appeared to have lower metabolic activity (Figure S4). Figure 6A outlines the timeline of the in situ stiffening experiments, including cell encapsulation, tyrosinase-mediated stiffening, and evaluations. On day-0, PSCs (1×10^6 cells/mL) were encapsulated in 2.5 wt% PEG8NB hydrogels crosslinked by either regular MMP-sensitive peptide (designated as 0Y, sequence: KCGPQGIWGQCK) or tyrosinase-MMP dually-sensitive peptide linker (2Y, Figure 4A). Evaluations were conducted at day-1 (prior to stiffening), day-3, and day-7. Because tyrosinase-mediated oxidation consumes dissolved oxygen (Figure 1D), we characterized the oxygen content in serum-containing PSC cell culture media where the stiffening occurred. As shown in Figure 6B, the oxygen content in both the control group (i.e., 0Y) and the experimental group (i.e., 2Y) were essentially identical throughout the course of the study. Although this enzymatic reaction consumes oxygen, no significant decrease in oxygen content was detected. This was most likely due to the fact that the reaction took place in a cell culture incubator where oxygen (21%) was allowed to freely diffuse into the media. The maintenance of oxygen content in the stiffened hydrogels implies that hypoxia would not be an issue affecting cell fate behavior in the stiffened hydrogels.

Figure 6C shows the pictures of the two sets of gels (0Y and 2Y) after treated with 1 kU/mL tyrosinase for 6 hours. From the top view, it can be seen that the size of the gel shrunk significantly in 2Y hydrogels, which were susceptible to tyrosinase-mediated stiffening. From the side view, however, the gel thickness remained roughly the same, suggesting that 2Y gels would be stiffer than the 0Y gels that were tyrosinase-insensitive. Live/dead staining and confocal imaging results revealed that almost all cells were viable in the hydrogels regardless of the stiffening conditions. Furthermore, there was higher degree of spreading in PSCs encapsulated in 0Y hydrogels than in 2Y gels (Figure 6D). The spreading of PSCs was quantified by measuring the aspect ratio of the cells encapsulated in 0Y and 2Y hydrogels (Figure 6E). Although the peptide crosslinker in both 0Y and 2Y hydrogels contained MMP-sensitive sequence, only 2Y hydrogels were susceptible to tyrosinase-mediated *in situ* stiffening. As a result, the degree of spreading of cells in stiffened 2Y hydrogels was significantly less than those in 0Y hydrogels. We also quantified the metabolic activity in the encapsulated PSCs using Alamarblue® reagent (Figure 6F). While both cell-laden hydrogels were treated with tyrosinase, only cells encapsulated in 2Y hydrogels showed reduced metabolic activity after the gels were stiffened by tyrosinase. It is worth noting that the reduction in metabolic activity was not due to cell death as most of the cells were still viable

as revealed by live/dead staining (Figure 6D). Together, these results demonstrate that the enzyme-mediated stiffening strategy was effective in affecting cell fate process in 3D. In a separate experiment, we performed *in situ* gel stiffening at day-3 post encapsulation (Figure 7A). In this case, cells were allowed to spread for three days prior to stiffening (Figure 7B, 7C). After stiffening with 1 kU/mL tyrosinase, the cells were further cultured for 4 days and results showed that while cells in non-stiffened (i.e., 0 kU/mL tyrosinase) hydrogels continued extending their cellular processes in 3D (Figure 7D, 7F), the spreading of cells after *in situ* stiffening was significantly hindered (Figure 7E, 7G). The effect of stiffening on cells was also observed in the metabolic activity (Figure S5A) and the aspect ratio (Figure S5B) of the cells.

In addition to cell morphology changes, we were interested in examining the molecular level changes in cells encapsulated in the stiffened hydrogels. We isolated mRNA from the cells and performed quantitative PCR (qPCR) on select genes that are known to be associated with the activation of PSCs, including α-smooth muscle actin (αSMA, Figure 8A), connective tissue growth factor (CTGF, Figure 8B), and hypoxia-inducible factor 1α (αSMA, Figure 8C). We found that the expression levels of αSMA were significantly higher in stiffened 2Y hydrogels than in 0Y hydrogels at day-7 post-encapsulation (i.e., day-6 post-stiffening). On the other hand, a significant difference in HIF1α expression was detected day-3 post-encapsulation (i.e., day-2 post-stiffening). The expression of CTGF in cells encapsulated in 0Y and 2Y hydrogels increased over time, but there was no statistical significant difference between the two groups.

We chose to detect the expression of αSMA, CTGF, and αSMA in encapsulated PSCs because these genes have been associated with myofibroblastic activation [38]. The increased expression of αSMA is a hallmark sign of myofibroblastic activation in many cells, such as hepatic stellate cells (HSCs) and valvular interstitial cells (VICs). Burdick and colleagues showed that αSMA expression was significantly higher when HSCs were cultured on the surface of stiff hydrogels [39, 40]. Accompanied with the increased expression of αSMA was the extensive spreading and protrusion of the cells. Differing from these earlier works, which were conducted on plannar gel surface, we encapsulated PSCs in 3D hydrogels with different stiffness. Although increased αSMA expression was detected (Figure 8A), the cell spreading in 3D was restricted due to a tightened network (Figure 6D). On the other hand, no statistical significant difference was found in the expression of CTGF between nonstiffened and stiffened matrices. Kwon et al. recently showed that the expression of CTGF in PSCs was significantly upregulated when the cells were treated with TGFβ [38]. Although both biochemical (e.g., TGFβ) and biophysical (e.g., matrix stiffness) signals are capable of activating stellate cells, the downstream molecular mechanisms involving these two environmental cues are different, and further studies are required. Lastly, we detected elevated HIF1α expression in PSCs encapsulated in stiffened gels (Figure 8C) and this result was not due to hypoxia (Figure 6B). Recent work has connected the relationship between increased expression of HIF1α in HSCs and the degree of liver fibrosis due to increased TGF-β signaling and EMT [41]. Other work on PSC showed that cellular stress, including hypoxia, could induce activation of PSCs [42]. Our results suggested that increased matrix stiffness, which can be considered a form of cellular stress, likely increased

the expression of HIF1α independent of oxygen tension in the system. Future mechanistic studies, however, are needed to test this hypothesis.

4. Conclusion

In summary, we have developed a dynamic hydrogel platform capable of undergoing on-demand and *in situ* gel stiffening by means of tyrosinase-mediated DOPA formation. Building upon the biomimetic features afforded by the diverse thiol-norbornene hydrogels, we designed simple peptide crosslinkers containing additional tyrosine residues for tyrosinase-mediated gel stiffening. Through exogenously adding tyrosinase, the hydrogels could be stiffened on-demand and with high controllability. The hydrogel system was cytocompatible for *in situ* cell encapsulation and the stiffening process did not induce cell damage. The stiffened hydrogel network restricted cell spreading and enhanced expression of genes relevant to myofibroblastic activation of PSCs, including αSMA and HIF1α. This hydrogel system provides an alternative stiffening strategy for *in situ* hydrogel stiffening without creating additional radicals during the stiffening process. Finally, the stiffening process takes hours to days to complete, and hence more closely mimics the actual tissue stiffening process *in vivo*. Future work will be focused on exploiting this stiffening strategy for molecular mechanisms related to the stiffening microenvironment found in pancreatic desmoplasia.

Supplementary Material

Refer to Web version on PubMed Central for supplementary material.

Acknowledgments

This work was supported by the National Cancer Institute of the NIH (R21CA188911).

References

1. Dupont S, Morsut L, Aragona M, Enzo E, Giulitti S, Cordenonsi M, Zanconato F, Le Digabel J, Forcato M, Bicciato S, Elvassore N, Piccolo S. Role of YAP/TAZ in mechanotransduction. Nature. 2011; 474:179–183. [PubMed: 21654799]
2. Gore J, Korc M. Pancreatic cancer stroma: Friend or foe? Cancer Cell. 2014; 25:711–712. [PubMed: 24937454]
3. Engler AJ, Sen S, Sweeney HL, Discher DE. Matrix elasticity directs stem cell lineage specification. Cell. 2006; 126:677–689. [PubMed: 16923388]
4. Tibbitt MW, Anseth KS. Hydrogels as extracellular matrix mimics for 3D cell culture. Biotechnol Bioeng. 2009; 103:655–663. [PubMed: 19472329]
5. Lin C-C, Anseth KS. PEG hydrogels for the controlled release of biomolecules in regenerative medicine. Pharm Res. 2009; 26:631–643. [PubMed: 19089601]
6. Yang C, Tibbitt MW, Basta L, Anseth KS. Mechanical memory and dosing influence stem cell fate. Nat Mater. 2014; 13:645–652. [PubMed: 24633344]
7. Kloxin AM, Kasko AM, Salinas CN, Anseth KS. Photodegradable hydrogels for dynamic tuning of physical and chemical properties. Science. 2009; 324:59–63. [PubMed: 19342581]
8. Khetan S, Guvendiren M, Legant WR, Cohen DM, Chen CS, Burdick JA. Degradation-mediated cellular traction directs stem cell fate in covalently crosslinked three-dimensional hydrogels. Nat Mater. 2013; 12:458–465. [PubMed: 23524375]

9. Mabry KM, Lawrence RL, Anseth KS. Dynamic stiffening of poly(ethylene glycol)-based hydrogels to direct valvular interstitial cell phenotype in a three-dimensional environment. Biomaterials. 2015; 49:47–56. [PubMed: 25725554]
10. Rosales AM, Mabry KM, Nehls EM, Anseth KS. Photoresponsive elastic properties of azobenzene-containing poly(ethylene-glycol)-based hydrogels. Biomacromolecules. 2015; 16:798–806. [PubMed: 25629423]
11. Stowers RS, Allen SC, Suggs LJ. Dynamic phototuning of 3D hydrogel stiffness. Proc Natl Acad Sci U S A. 2015; 112:1953–1958. [PubMed: 25646417]
12. Shih H, Lin C-C. Tuning stiffness of cell-laden hydrogels via host-guest interactions. Journal of Materials Chemistry B. 2016 In press.
13. Jonker AM, Borrmann A, Van Eck ER, Van Delft FL, Lowik DW, Van Hest JC. A fast and activatable cross-linking strategy for hydrogel formation. Adv Mater. 2015; 27:1235–1240. [PubMed: 25535032]
14. Das S, Pati F, Choi YJ, Rijal G, Shim JH, Kim SW, Ray AR, Cho DW, Ghosh S. Bioprintable, cell-laden silk fibroin-gelatin hydrogel supporting multilineage differentiation of stem cells for fabrication of three-dimensional tissue constructs. Acta Biomater. 2015; 11:233–246. [PubMed: 25242654]
15. Mosiewicz KA, Kolb L, Van Der Vlies AJ, Martino MM, Lienemann PS, Hubbell JA, Ehrbar M, Lutolf MP. In situ cell manipulation through enzymatic hydrogel photopatterning. Nat Mater. 2013; 12:1072–1078. [PubMed: 24121990]
16. Anjum F, Lienemann PS, Metzger S, Biernaskie J, Kallos MS, Ehrbar M. Enzyme responsive GAG-based natural-synthetic hybrid hydrogel for tunable growth factor delivery and stem cell differentiation. Biomaterials. 2016; 87:104–117. [PubMed: 26914701]
17. Wang LS, Du C, Chung JE, Kurisawa M. Enzymatically cross-linked gelatin-phenol hydrogels with a broader stiffness range for osteogenic differentiation of human mesenchymal stem cells. Acta Biomater. 2012; 8:1826–1837. [PubMed: 22343003]
18. Land EJ, Ramsden CA, Riley PA. Tyrosinase autoactivation and the chemistry of orthoquinone amines. Accounts of chemical research. 2003; 36:300–308. [PubMed: 12755639]
19. Lim KS, Alves MH, Poole-Warren LA, Martens PJ. Covalent incorporation of non-chemically modified gelatin into degradable PVA-tyramine hydrogels. Biomaterials. 2013; 34:7097–7105. [PubMed: 23800741]
20. Lin C-C, Ki CS, Shih H. Thiol-norbornene photoclick hydrogels for tissue engineering applications. Journal of Applied Polymer Science. 2015; 132:41563. [PubMed: 25558088]
21. Fairbanks BD, Schwartz MP, Halevi AE, Nuttelman CR, Bowman CN, Anseth KS. A versatile synthetic extracellular matrix mimic via thiol-norbornene photopolymerization. Adv Mater. 2009; 21:5005–5010. [PubMed: 25377720]
22. Lustig SR, Peppas NA. SOLUTE DIFFUSION IN SWOLLEN MEMBRANES .9. SCALING LAWS FOR SOLUTE DIFFUSION IN GELS. Journal of Applied Polymer Science. 1988; 36:735–747.
23. Raza A, Lin C-C. The Influence of Matrix Degradation and Functionality on Cell Survival and Morphogenesis in PEG-Based Hydrogels. Macromol Biosci. 2013; 13:1048–1058. [PubMed: 23776086]
24. Fairbanks BD, Schwartz MP, Bowman CN, Anseth KS. Photoinitiated polymerization of PEG-diacrylate with lithium phenyl-2,4,6-trimethylbenzoylphosphinate: polymerization rate and cytocompatibility. Biomaterials. 2009; 30:6702–6707. [PubMed: 19783300]
25. Tibbitt MW, Kloxin AM, Sawicki LA, Anseth KS. Mechanical Properties and Degradation of Chain and Step-Polymerized Photodegradable Hydrogels. Macromolecules. 2013; 46:2785–2792.
26. Bell CL, Peppas NA. Water, solute and protein diffusion in physiologically responsive hydrogels of poly(methacrylic acid-g-ethylene glycol). Biomaterials. 1996; 17:1203–1218. [PubMed: 8799505]
27. Mellott MB, Searcy K, Pishko MV. Release of protein from highly cross-linked hydrogels of poly(ethylene glycol) diacrylate fabricated by UV polymerization. Biomaterials. 2001; 22:929–941. [PubMed: 11311012]
28. Sharma RC, Ali R. Hydrodynamic properties of mushroom tyrosinase. Phytochemistry. 1981; 20:399–401.

29. Behbahani I, Miller SA, Okeeffe DH. A COMPARISON OF MUSHROOM TYROSINASE DOPAQUINONE AND DOPACHROME ASSAYS USING DIODE-ARRAY SPECTROPHOTOMETRY - DOPACHROME FORMATION VS ASCORBATE-LINKED DOPAQUINONE REDUCTION. Microchemical Journal. 1993; 47:251–260.
30. Lutolf MP, Hubbell JA. Synthetic biomaterials as instructive extracellular microenvironments for morphogenesis in tissue engineering. Nat Biotechnol. 2005; 23:47–55. [PubMed: 15637621]
31. Lin C-C. Recent advances in crosslinking chemistry of biomimetic poly(ethylene glycol) hydrogels. RSC advances. 2015; 5:39844–398583. [PubMed: 26029357]
32. Lin T-Y, Ki CS, Lin C-C. Manipulating hepatocellular carcinoma cell fate in orthogonally crosslinked hydrogels. Biomaterials. 2014; 35:6898–6906. [PubMed: 24857292]
33. Ki CS, Lin T-Y, Korc M, Lin C-C. Thiol-ene hydrogels as desmoplasia-mimetic matrices for modeling pancreatic cancer cell growth, invasion, and drug resistance. Biomaterials. 2014; 35:9668–9677. [PubMed: 25176061]
34. Lin C-C, Raza A, Shih H. PEG hydrogels formed by thiol-ene photo-click chemistry and their effect on the formation and recovery of insulin-secreting cell spheroids. Biomaterials. 2011; 32:9685–9695. [PubMed: 21924490]
35. Greene T, Lin C-C. Modular cross-linking of gelatin-based thiol-norbornene hydrogels for in vitro 3D culture of hepatocellular carcinoma cells. ACS Biomaterials Science & Engineering. 2015; 1:1314–1323.
36. Kikuta K, Masamune A, Watanabe T, Ariga H, Itoh H, Hamada S, Satoh K, Egawa S, Unno M, Shimosegawa T. Pancreatic stellate cells promote epithelial-mesenchymal transition in pancreatic cancer cells. Biochemical and Biophysical Research Communications. 2010; 403:380–384. [PubMed: 21081113]
37. Luo G, Long J, Zhang B, Liu C, Xu J, Ni Q, Yu X. Stroma and pancreatic ductal adenocarcinoma: An interaction loop. Biochimica Et Biophysica Acta-Reviews on Cancer. 2012; 1826:170–178.
38. Kwon JJ, Nabinger SC, Vega Z, Sahu SS, Alluri RK, Abdul-Sater Z, Yu Z, Gore J, Nalepa G, Saxena R, Korc M, Kota J. Pathophysiological role of microRNA-29 in pancreatic cancer stroma. Scientific reports. 2015; 5:11450. [PubMed: 26095125]
39. Guvendiren M, Perepelyuk M, Wells RG, Burdick JA. Hydrogels with differential and patterned mechanics to study stiffness-mediated myofibroblastic differentiation of hepatic stellate cells. Journal of the mechanical behavior of biomedical materials. 2014; 38:198–208. [PubMed: 24361340]
40. Caliari SR, Perepelyuk M, Soulas EM, Lee GY, Wells RG, Burdick JA. Gradually softening hydrogels for modeling hepatic stellate cell behavior during fibrosis regression. Integrative biology : quantitative biosciences from nano to macro. 2016; 8:720–728. [PubMed: 27162057]
41. Kim MJ, Park SA, Kim CH, Park SY, Kim JS, Kim DK, Nam JS, Sheen YY. TGF-beta Type I Receptor Kinase Inhibitor EW-7197 Suppresses Cholestatic Liver Fibrosis by Inhibiting HIF1alpha-Induced Epithelial Mesenchymal Transition. Cellular physiology and biochemistry : international journal of experimental cellular physiology, biochemistry, and pharmacology. 2016; 38:571–588.
42. Rebours V, Albuquerque M, Sauvanet A, Ruszniewski P, Levy P, Paradis V, Bedossa P, Couvelard A. Hypoxia pathways and cellular stress activate pancreatic stellate cells: development of an organotypic culture model of thick slices of normal human pancreas. PLoS One. 2013; 8:e76229. [PubMed: 24098783]

Statement of Significance

Hydrogels with spatial-temporal controls over crosslinking kinetics (i.e., dynamic hydrogel) are increasingly being developed for studying mechanobiology in 3D. The general principle of designing dynamic hydrogel is to perform cell encapsulation within a hydrogel network that allows for post-gelation modification in gel crosslinking density. The enzyme-mediated *in situ* gel stiffening is innovative because of the specificity and efficiency of enzymatic reaction. Although tyrosinase has been used for hydrogel crosslinking and *in situ* cell encapsulation, to the best of our knowledge tyrosinase-mediated DOPA formation has not been explored for *in situ* stiffening of cell-laden hydrogels. Furthermore, the current work provides a gradual matrix stiffening strategy that may more closely mimic the process of tumor development.

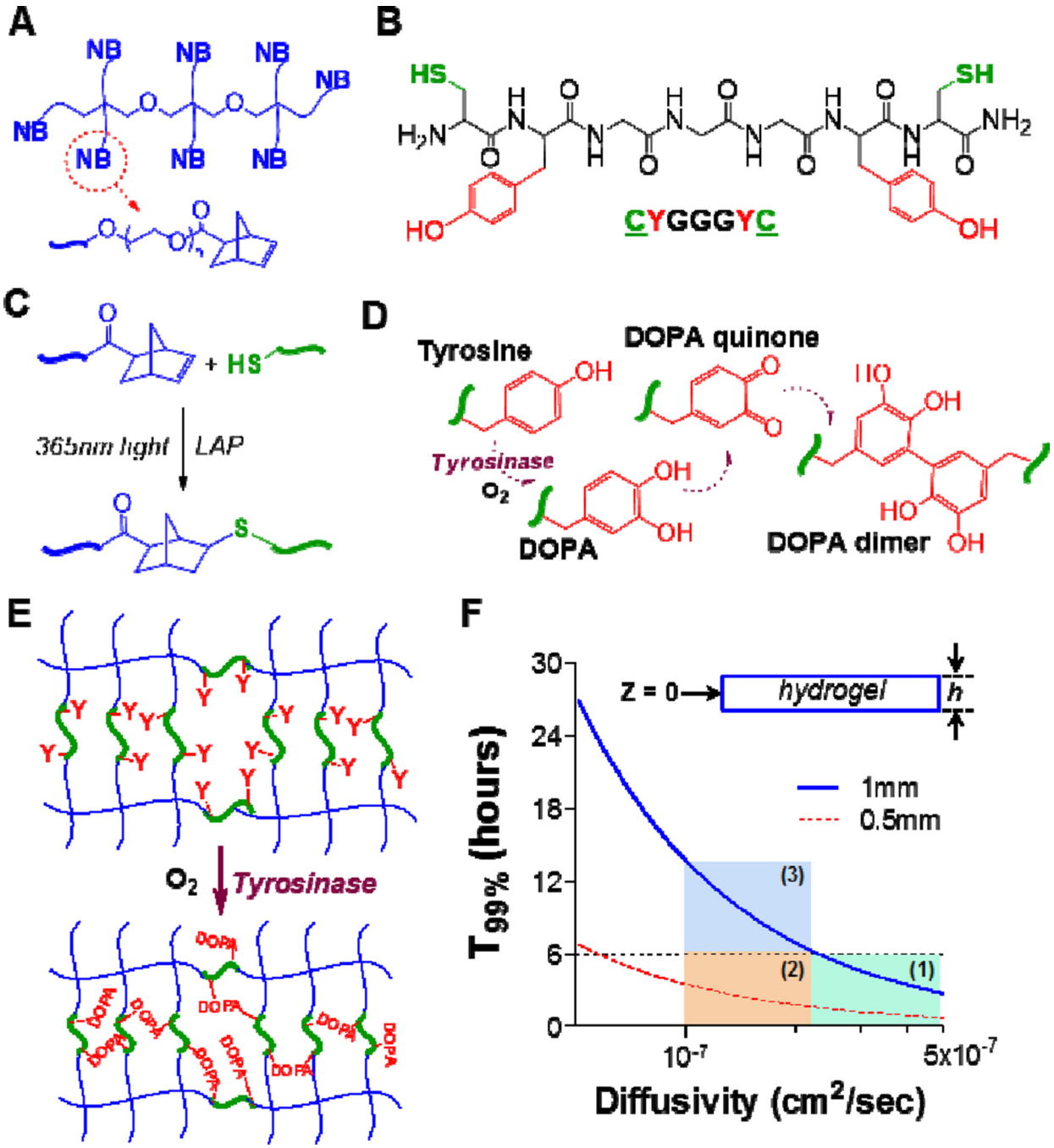

Figure 1. Schematics of thiol-norbornene hydrogels susceptible to tyrosinase-mediated *in situ* gel stiffening

(A) Structure of 8-arm poly(ethylene glycol)-norbornene (PEG8NB). (B) Model bis-cysteine-bis-tyrosine peptide crosslinker CYGGGYC. (C) Light mediated thiol-norbornene photoclick reaction to form PEG8NB-peptide hydrogel. 1 mM LAP was used as the photoinitiator. (D) Tyrosinase-mediated oxidation of tyrosine into DOPA, DOPA quinone, and DOPA dimer. (E) PEG8NB-peptide hydrogel bearing pendant tyrosines for tyrosinase-mediated DOPA dimer formation that leads to increased gel crosslinking density. (F) Prediction of $T_{99\%}$ (i.e., $C_{z=0} \geq 0.99 \times C_{z=h}$) in a disc-shape hydrogel with a thickness of *h*.

Regions 1–3 represent scenarios for which a period of 6-hr tyrosinase incubation are sufficient (regions 1 & 2) or insufficient (region 3) to fulfill the criterion of $C_{z=0} \geq 0.99 \times C_{z=h}$.

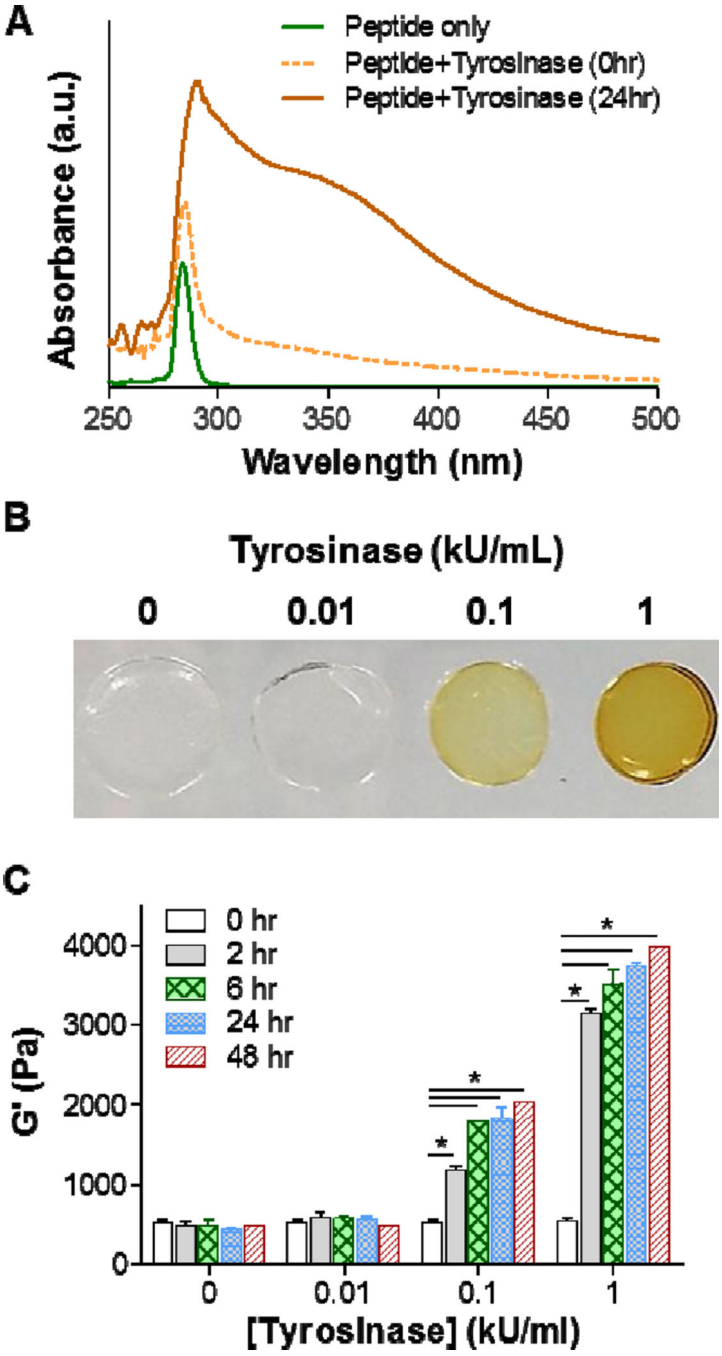

Figure 2. Tyrosinase-mediated *in situ* stiffening of PEG-based hydrogels

(A) UV/Vis absorbance spectrum of 5 mM CYGGGYC peptide, peptide/tyrosinase (1 kU/mL) mixture before (0hr) and after 24hr incubation. (B) Photographs of PEG-peptide (i.e., 2.5wt% PEG8NB, 5 mM CYGGGYC) hydrogels treated with different concentrations of tyrosinase. (C) Effect of tyrosinase concentration of shear moduli (G') of the PEG-peptide hydrogels. Crosslinked hydrogels were incubated in PBS for one day prior to 6hr of tyrosinase treatment. Afterward, the gels were transferred to PBS and gel moduli were

monitored periodically using oscillatory rheometer. Data represent Mean ± SEM (n = 3). Asterisks indicate $p<0.05$ (compared with gels at 0hr, i.e., prior to tyrosinase treatment).

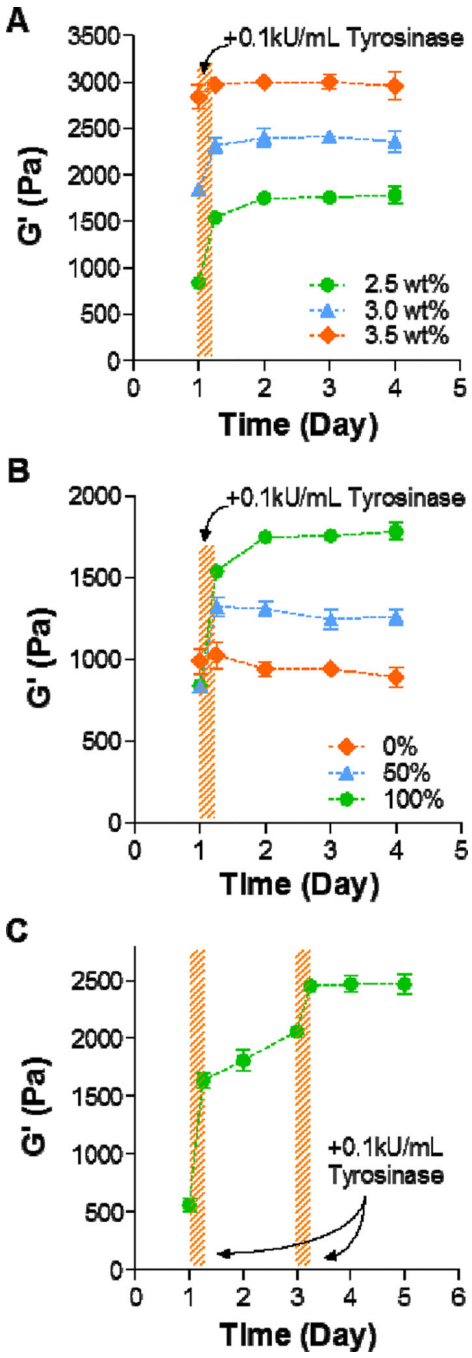

Figure 3. Controlling the degree of *in situ* gel stiffening

(A) Effect of PEG8NB weight percent (2.5, 3.0, and 3.5 wt%) on the degree of gel stiffening. The concentration of CYGGGYC was adjusted such that a stoichiometric ratio of thiol-to-ene moieties was maintained (i.e., 5, 6, and 7 mM peptide, respectively). Hydrogels were allowed to swell for one day post-gelation, followed by tyrosinase treatment for 6 hours (shaded area). (B) Effect of tyrosinase-sensitive peptide content on the degree of *in situ* gel stiffening. PEG8NB content was fixed at 2.5wt%, whereas tyrosinase-sensitive (i.e., CYGGGYC) and insensitive (i.e., CGGGC) peptide crosslinkers were mixed at different

percentages (0, 50, and 100% CYGGGYC). (C) Temporal control in gel stiffening. Swollen hydrogels (2.5wt% PEG8NB and 5 mM CYGGGYC) were treated with tyrosinase at day 1 for 3 hours and again at day 3 for another 3 hours. Data represent Mean ± SEM (n = 3).

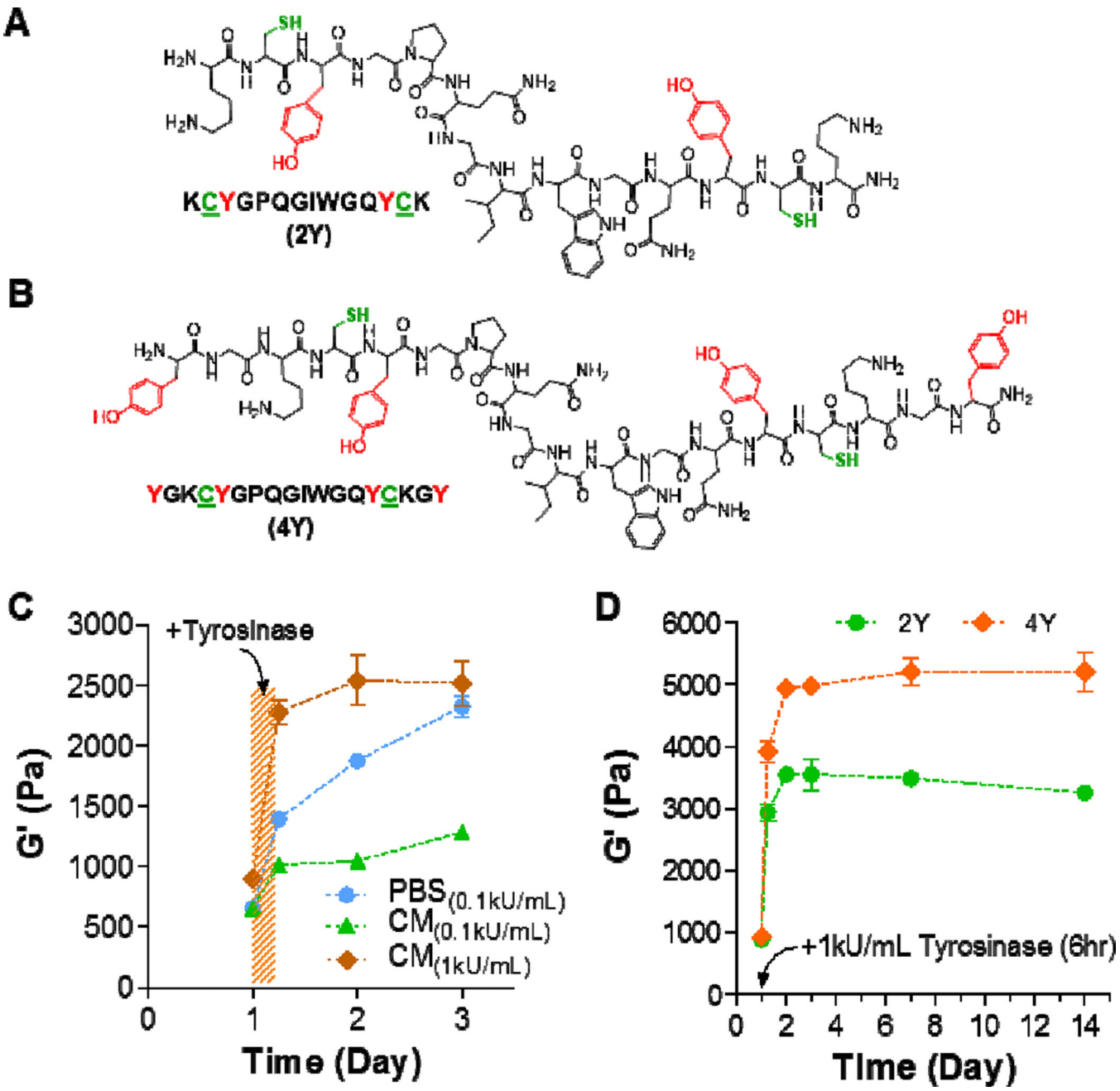

Figure 4. ***In situ*** **stiffening of MMP-sensitive PEG8NB-peptide hydrogels**

(A, B) Chemical structures of bis-cysteine MMP-sensitive peptide crosslinker bearing additional two (A) or four (B) tyrosine residues for tyrosinase-mediated gel stiffening. (C) Effect of solution composition on elastic moduli of *in situ* stiffened PEG-peptide hydrogels. CM: PSC culture media. Gel formulation: 2.5wt% PEG8NB with 2Y peptide. (D) Effect of tyrosine residues (2 or 4 tyrosines) on elastic moduli of *in situ* stiffened PEG-peptide hydrogels (2.5wt% PEG8NB). Data represent Mean ± SEM (n = 3).

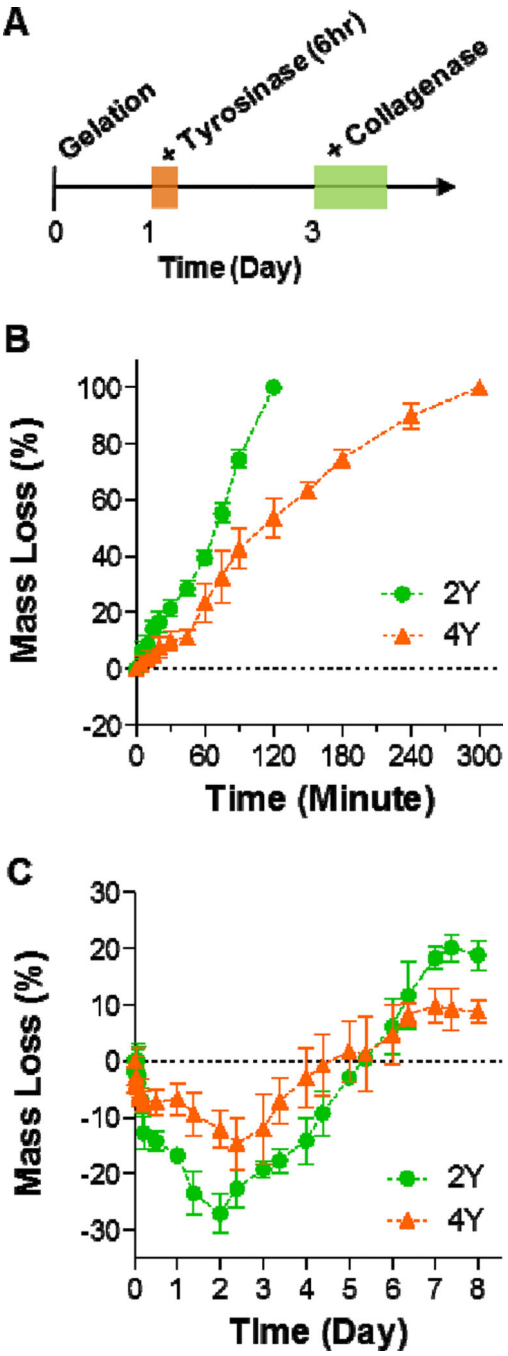

Figure 5. Proteolytic degradation of MMP-sensitive PEG8NB-peptide hydrogels

(A) Timeline of the study. (B, C) Collagenase-mediated mass loss of non-stiffened hydrogels (B) and tyrosinase-stiffened hydrogels (C). All gels were formed with 2.5wt% PEG8NB with 5 mM MMP-sensitive peptide (2Y or 4Y). Data represent Mean ± SEM (n = 3).

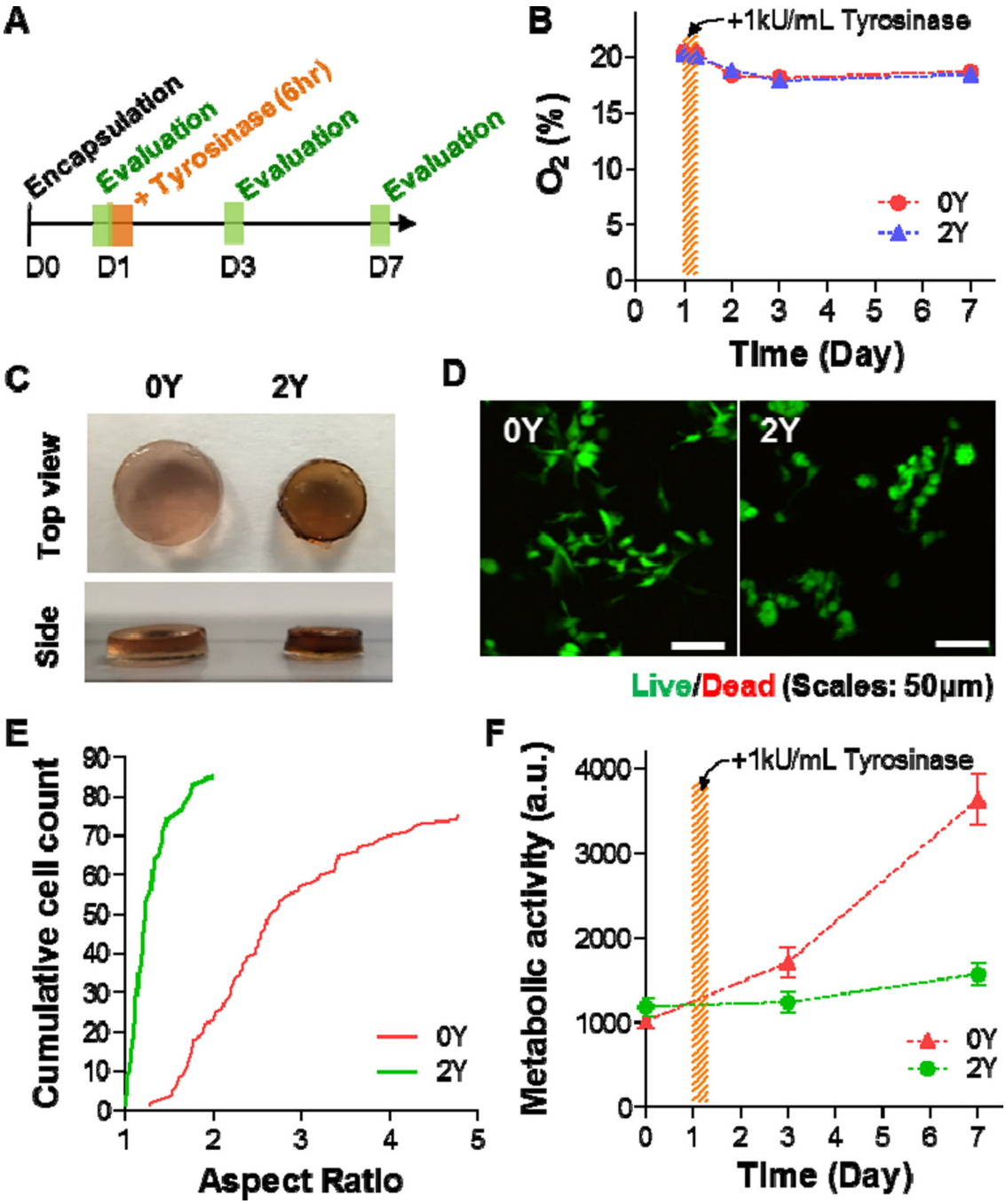

Figure 6. Effect of matrix stiffening on pancreatic stellate cell fate in 3D

(A) Timeline of the study. (B) Oxygen contents in PSC culture media with 0Y or 2Y PEG-peptide hydrogels. Tyrosinase-mediated stiffening was conducted on day-1 for 6hr. (C) Photographs of cell-laden hydrogels crosslinked by 0Y or 2Y MMP-sensitive peptide. (D) Representative confocal z-stack images of live/dead stained PSCs encapsulated in 0Y or 2Y MMP-sensitive PEG-peptide hydrogels. (E) Aspect ratio of encapsulated PSCs at day-7 post-encapsulation. (F) Metabolic activity of encapsulated PSCs. All gels were treated with 1 kU/mL tyrosinase at day-1 post-encapsulation. Data represent Mean ± SEM (n = 3).

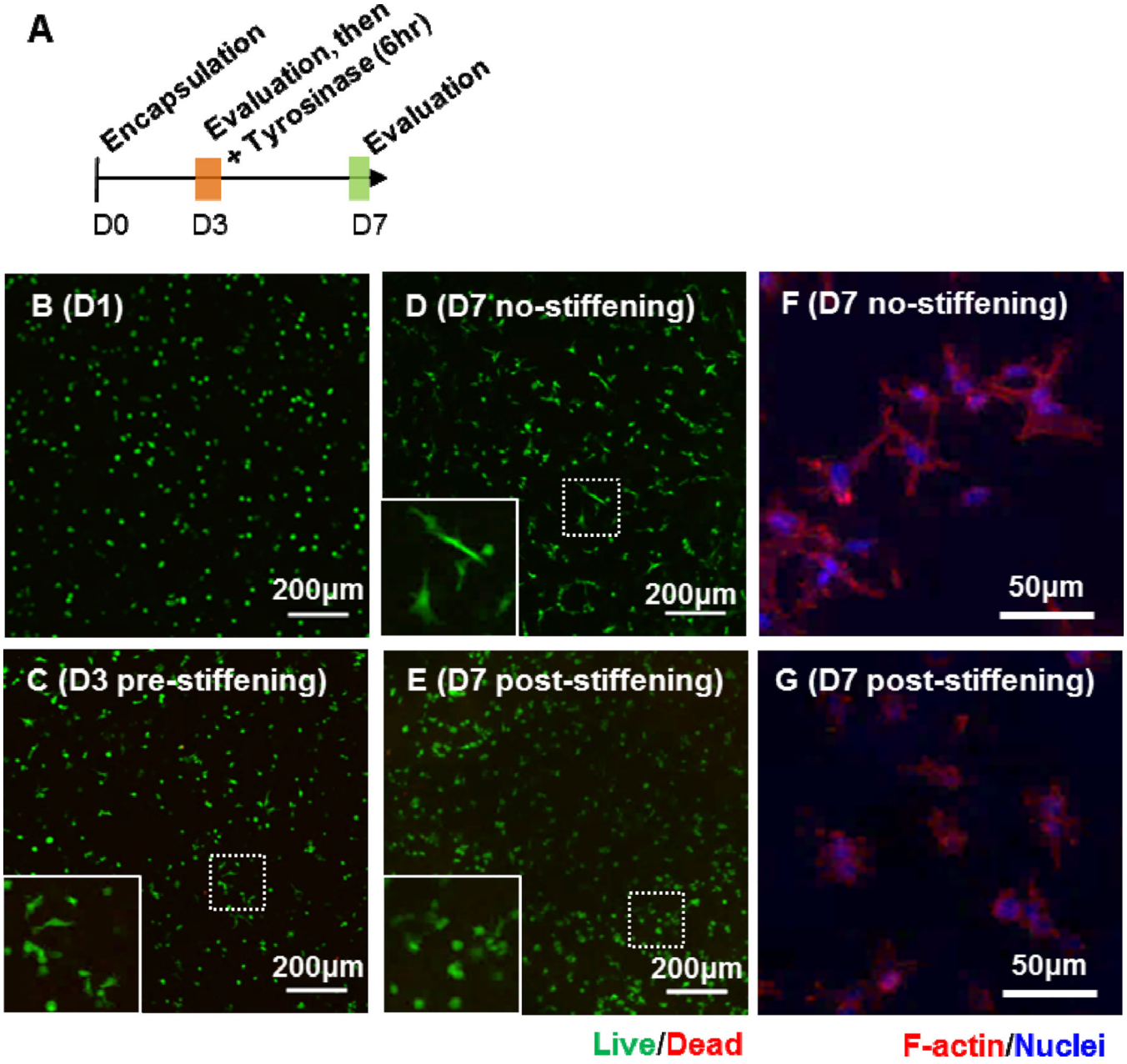

Figure 7.

(A) Timeline of the study. (B–E) Representative confocal z-stack images of live/dead stained PSCs encapsulated in PEG-peptide hydrogels at day-1 (B), day-3 before stiffening (C), day-7 without stiffening (D), and day-7 with stiffening (E). Representative confocal z-stack images of F-actin stained PSCs at day-7 without (F) and with stiffening (G).

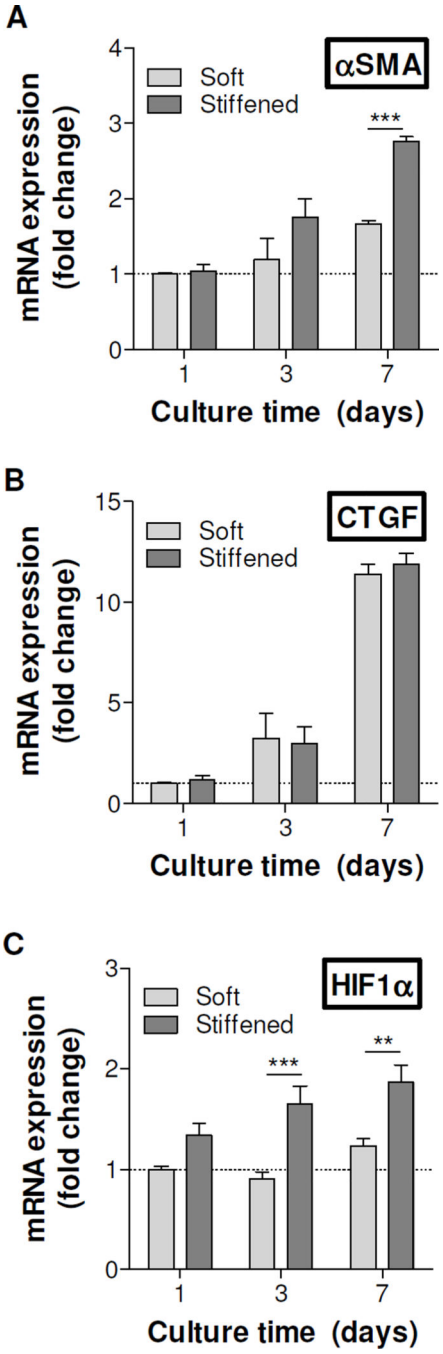

Figure 8. Effect of matrix stiffening on gene expression in pancreatic stellate cells

mRNA samples were collected from cell-laden hydrogels before stiffening (day-1), as well as day-2 and day-6 post-stiffening using 1 kU/mL tyrosinase (i.e., day-3, day-7 culture time). Soft: Cell-laden hydrogels crosslinked by regular MMP-sensitive peptide (i.e., 0Y peptide). Stiffened: Cell-laden hydrogels crosslinked by 2Y peptide. GAPDH was used as the housekeeping gene and the expression levels of αSMA (A), CTGF (B), and HIF1α (C) in different samples were normalized to that in day-1 soft gel (1-fold). Experiments were

repeated independently for three times with three samples in each group. (Data represent Mean ± SEM). **p<0.01, ***p<0.001.